Integrated All-Light Network for Air, Space, Land, and Sea

LIANG Yingze[1,2], WANG Linning[1,2], QI Ziqian[1], LIU Pengzhan[1], WANG Yongjin[1]
(1. GaN Optoelectronic Integration International Cooperation Joint Laboratory of Jiangsu Province, Nanjing 210003, China;
2. Nanjing University of Posts and Telecommunications, Nanjing 210003, China)

DOI: 10.12142/ZTECOM.202502012
https://kns.cnki.net/kcms/detail/34.1294.TN.20250512.1406.004.html, published online May 13, 2025
Manuscript received: 2024-12-10

Abstract: To meet the demands of high-speed communication under strong electromagnetic interference, an all-light network (ALN) based on a multi-band optical communication system is proposed. It is designed for cross-scenario interconnection and networking, covering air, space, land, and sea. The ALN integrates four types of optical links: underwater blue light communication, white light illumination communication, solar-blind deep ultraviolet communication, and long-distance laser communication systems. These links are interconnected via Ethernet switches with the Transmission Control Protocol (TCP). Any ALN node supports both wired and wireless device access. The data transmission performance between network nodes was tested, with a maximum transmission delay of 73.3 ms, a maximum packet loss rate of 6.1%, and a maximum jitter of 15 ms. This comprehensive all-light network with all-scenario coverage lays the foundation for the future development of network technologies and the digital economy.

Keywords: all-light network; multi-band optical communication system; Ethernet switches

Citation (Format 1): LIANG Y Z, WANG L N, QI Z Q, et al. Integrated all-light network for air, space, land, and sea [J]. ZTE Communications, 2025, 23(2): 109–114. DOI: 10.12142/ZTECOM.202502012
Citation (Format 2): Y. Z. Liang, L. N. Wang, Z. Q. Qi, et al., "Integrated all-light network for air, space, land, and sea," *ZTE Communications*, vol. 23, no. 2, pp. 109–114, Jun. 2025. doi: 10.12142/ZTECOM.202502012.

1 Introduction

In the contemporary field of communications, optical communication, as an emerging and rapidly advancing technology, is increasingly becoming an integral component of future communication networks[1–8]. Wireless optical communication offers high-speed and low-latency data transmission and unique advantages in complex and denied environments as a complementary communication method.

An all-light network (ALN) represents the culmination of optical communication technologies. It integrates white light illumination communication (WLC), underwater blue light communication (BLC), solar-blind deep ultraviolet communication (DUVC), and long-distance laser communication (LC). This work focuses on the ALN and aims to develop a highly efficient optical communication network with multispectral capabilities and comprehensive scene coverage.

Compared to radio frequency (RF) networks, the ALN demonstrates significant performance advantages. Firstly, it offers excellent anti-interference capability, as optical signals are unaffected by electromagnetic environments[9]. With high directionality, interference resistance, and enhanced security, the ALN is particularly suitable for complex or constrained environments. Secondly, its bandwidth is far superior to that of RF networks, enabling large-capacity data transmission to meet the demands of future ultra-high-speed networks. Lastly, its low latency characteristics make it exceptionally well-suited for scenarios requiring high real-time performance. Leveraging these features, the ALN not only extends the application scope of communication networks but also provides a substantial performance boost to traditional communication methods. It can be employed in disaster emergency communications, deep-sea and space communications, and industrial automation, among other scenarios.

As shown in Fig. 1, there are four main practical application scenarios for full-spectrum optical communication: illumination communication, underwater communication, solar-blind communication, and long-distance communication. We develop subsystems for each scenario using light-emitting di-

This work was supported by the National Natural Science Foundation of China under Grant No. U21A20495, Research and Development Program of China under Grant No. 2022YFE0112000, and Higher Education Discipline Innovation Project under Grant No. D17018.
The authors contributed equally to this work.

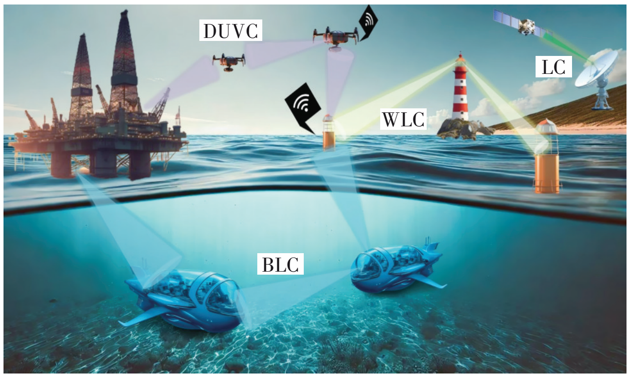

BLC: blue light communication
DUVC: deep ultraviolet communication
LC: laser communication
WLC: white light illumination communication

Figure 1. All-light network (ALN) applications spanning air, space, land and sea

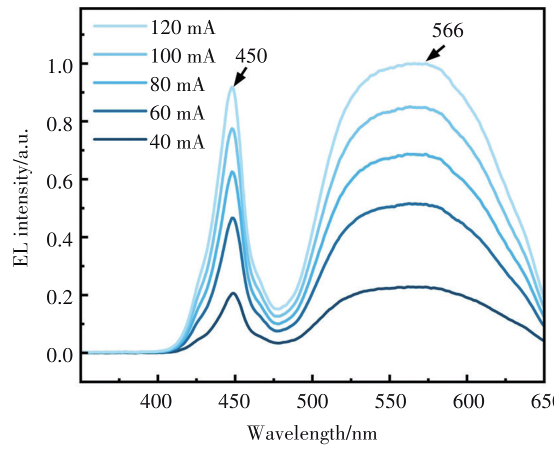

EL: electroluminescence

Figure 2. Electroluminescence spectra variation of white LED in white light illumination communication with increasing injection currents

odes (LEDs) or laser diodes (LDs) operating across four distinct spectral bands. WLC provides efficient data transmission and serves a dual role in illumination. For instance, WLC between buoys and lighthouses enables simultaneous information transmission. Blue and green light exhibit minimal loss in pure seawater, allowing for long-range data transmission[10–13]. BLC facilitates reliable data transfer in underwater environments, enabling control of uncrewed underwater vehicles or establishing communication between underwater sensors and buoys. Due to the ozone layer's absorption, background noise in the deep ultraviolet spectrum is extremely low at the Earth's surface, making DUVC suitable for environments with strong light or electromagnetic interference[14]. Meanwhile, long-distance LC, with its high-power directed beams, provides robust support for long-range, high-bandwidth communication, such as point-to-point communication in space[15]. By using Ethernet switches (ESes) combined with Wireless Fidelity (Wi-Fi) technology or optical fiber technology to connect various optical communication links, the ALN enables information sharing among different network nodes.

2 Experiments and Discussion

In our experiments, we characterized the white LED's electroluminescence (EL) spectra for WLC using a Keithley 2636B SourceMeter and an Ocean Optics HR4000 spectrometer. A multimode optical fiber with a diameter of 200 μm was used to collect the light emitted by the white LED under different injection currents and transmit it to the HR4000 spectrometer. The results are shown in Fig. 2. The EL spectrum of the white LED exhibits a distinct dual-peak profile, with the blue emission peak and excitation peak appearing from left to right. As the injection current increases from 40 mA to 120 mA, the blue emission peak shifts from 449.1 nm to 448 nm, corresponding to a blue shift of 1.1 nm. Meanwhile, the excitation peak remains stable at 566 nm.

We utilized a Keysight E5080A network analyzer to pulse the white LED using an alternating current (AC) signal, generating a bias voltage through a bias-tee module. The modulated light was captured by a Hamamatsu C12702-11 photodiode module and fed back to an Agilent Technologies PNA-LN5203C network analyzer for 3 dB processing. The results are shown in Fig. 3a. When the bias voltage increases from 10.5 V to 12 V, the 3 dB bandwidth expands from 0.55 MHz to 1.13 MHz. However, at a bias voltage of 12.5 V, the bandwidth decreases to 1.02 MHz, likely due to thermal effects in the white LED during actual operation. Therefore, we selected a bias voltage of 12 V to achieve a higher communication rate. This method was also applied to LEDs or LDs operating in other spectral bands. As shown in Fig. 3b, the 3 dB bandwidth of the blue LED reaches a maximum of 4.68 MHz under a driving voltage of 12 V. Fig. 3c presents the 3 dB performance characterization of the green LD device, which achieves a 3 dB bandwidth of 20.2 MHz at a bias voltage of 6 V, indicating that the green LD can achieve a higher modulation rate. As shown in Fig. 3d, the 3 dB bandwidth of the deep-ultraviolet (DUV) LED reaches 25.2 MHz at an operating voltage of 5.6 V. This indicates that the DUV LED theoretically achieves the highest modulation rate among the four types of devices.

We constructed an all-light communication network spanning space, air, and ocean using four different spectral bands: 278 nm, 450 nm, 520 nm, and 566 nm, as shown in Fig. 4. The WLC system is suitable for indoor and outdoor environments. The underwater BLC system addresses the challenges of underwater communication. The DUVC system ensures stable communication under strong illumination conditions, while the long-distance LC system meets the requirements for long-range, high-bandwidth communications.

The testing results showed that WLC achieved a communication rate of at least 2 Mbit/s over a 200 m ground communica-

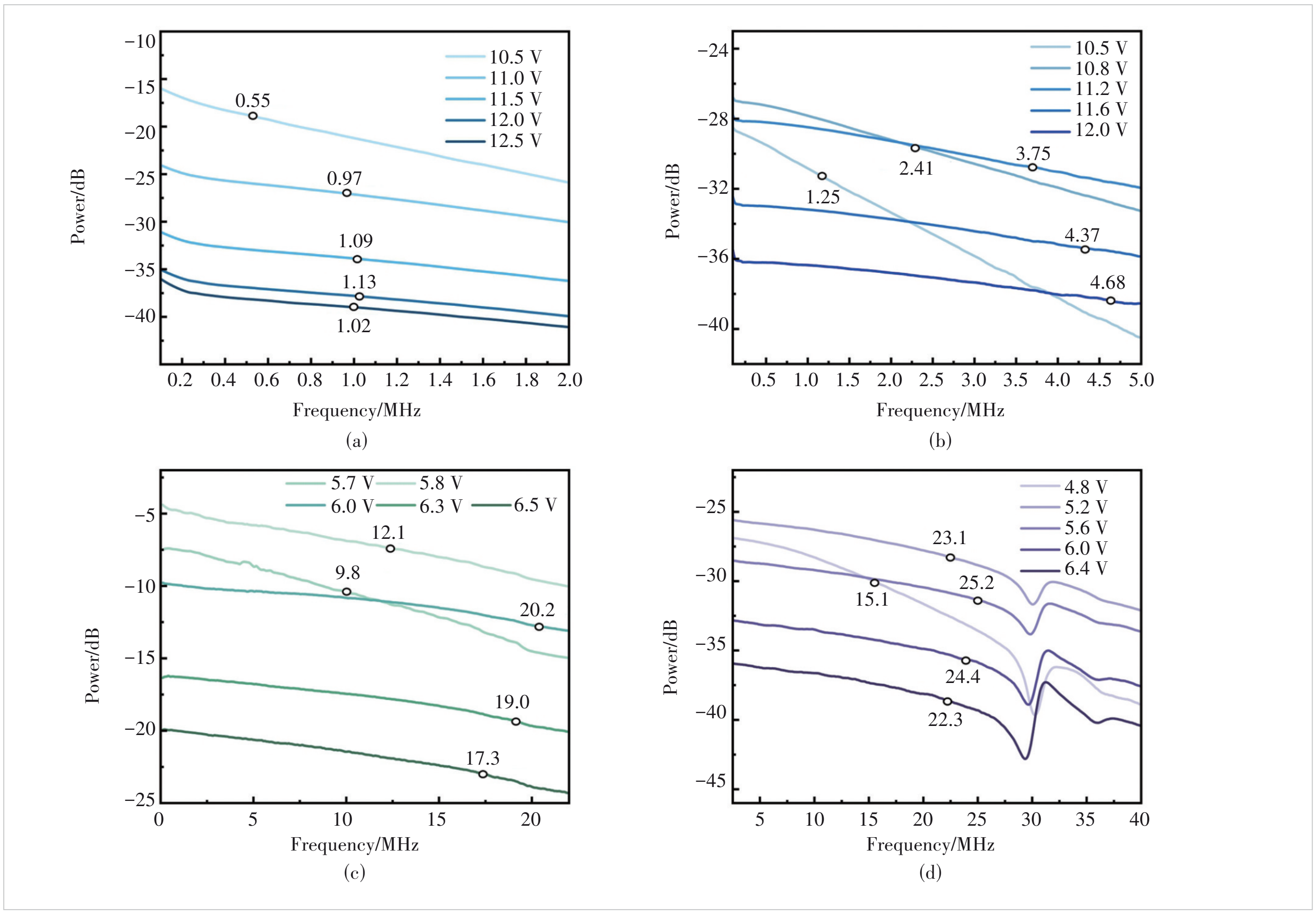

Figure 3. (a) 3 dB bandwidth variation of the white LED with increasing offset voltages; (b) 3 dB bandwidth variation of the blue LED with increasing offset voltages; (c) 3 dB bandwidth variation of the green LD with increasing offset voltages; (d) 3 dB bandwidth variation of the deep-ultraviolet LED with increasing offset voltages

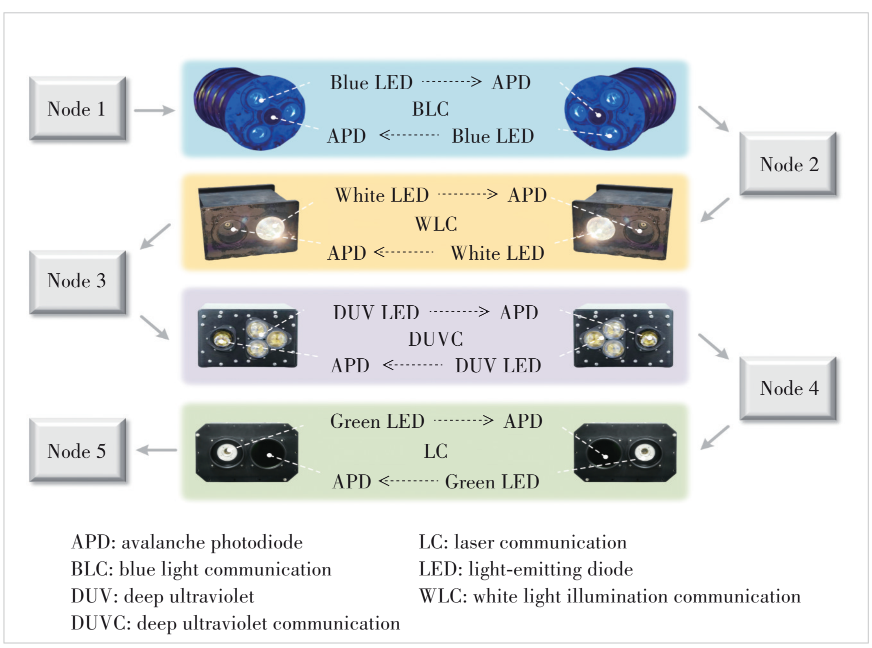

Figure 4. Schematic of the proposed all-light network (ALN) framework

tion distance. Underwater conditions featuring an attenuation coefficient of 0.4 dB/m, BLC supported full-duplex optical communication over distances of at least 50 m, with a communication rate of at least 4 Mbit/s. Both DUVC and LC achieved a communication rate of 10 Mbit/s, with tested distances of 10 m and 120 m, respectively.

By integrating multiple technologies, the ALN system enables flexible configurations and robust adaptability across diverse environments. Whether encountering extreme weather conditions, complex terrains, or specialized application scenarios, the ALN system delivers stable and reliable communication services.

ALN comprises four full-duplex wireless optical communication links connected in series through five nodes. These nodes are formed by ESes, enabling communication systems operating in different spectral bands to establish networks with optical fibers, even in denied environments with heavy electromagnetic interference. Devices such as sensors, cameras, and PCs can access the ALN at any node through ESes. Additionally, Wi-Fi modules can be integrated into the nodes to provide wireless data access services for PCs and mobile devices, further expanding the ALN's connectivity options. The ESes can be expanded to accommodate multiple devices at the same node. To standardize transmission, all nodes in the wireless optical communication link use Registered Jack-45 (RJ45) network interfaces.

All four optical communication links operate in the full-duplex mode. The demonstration of the signal flow is shown in Fig. 5. When the underwater network camera captures video and sends it to Node 1 (N1), the video signal is encoded into a blue light signal by the BLC transmitter. At the BLC receiver, the light is filtered through a lens using a narrowband filter with a central wavelength of 450 nm, a half-bandwidth of 10 nm, and 45% transmittance, isolating the communication signal from ambient light. Each receiving end of the optical communication systems in different spectral bands is equipped with a corresponding narrowband filter. The optical signal is converted into an electrical signal by an avalanche photodiode (APD), then decoded by the BLC receiver and transmitted to N2. Subsequently, the signal is transmitted via the WLC link using illumination communication with a central wavelength of 566 nm. The signal at N3 is then transmitted to the next node via DUVC. Finally, the LC system converts the signal from N4 into a laser signal, and after transmission through the laser link, the original video stream is restored.

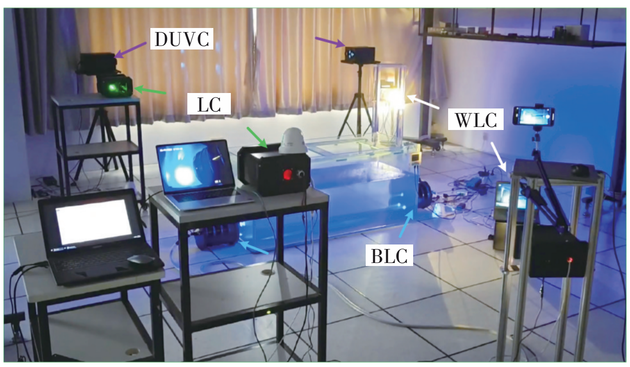

BLC: blue light communication
DUVC: deep ultraviolet communication
LC: laser communication
WLC: white light illumination communication

Figure 5. Demonstration of signal flow in all-light network (ALN)

The full-duplex optical communication system comprises a transmitter (TX) and a receiver (RX). The schematic diagram of the transmission and reception principles is shown in Fig. 6. In the transmission processing chain, a network camera or other sensor using the Transmission Control Protocol (TCP) is connected to the ES via an RJ45 interface. The video stream is then progressively converted into an optical signal. The core components of the TX are LEDs or LDs operating in different spectral bands. The direct current (DC) signal is supplied by an external LM2587 module, while the RF signal is synchronously generated by a transistor-transistor logic (TTL) signal using on-off keying (OOK) modulation within the field-programmable gate array (FPGA) main processing unit (Xilinx Spartan 6). The TTL signal drives the metal-oxide-semiconductor field-effect transistor (MOSFET) or bias tee via the PMD2001D driver. Finally, the modulated optical signal is emitted by the LED or LD.

The RX utilizes a high-sensitivity APD as the core component in the reception processing chain. The APD receives the optical signal under high voltage and converts it into a photocurrent. After amplification and filtering, the signal is re-

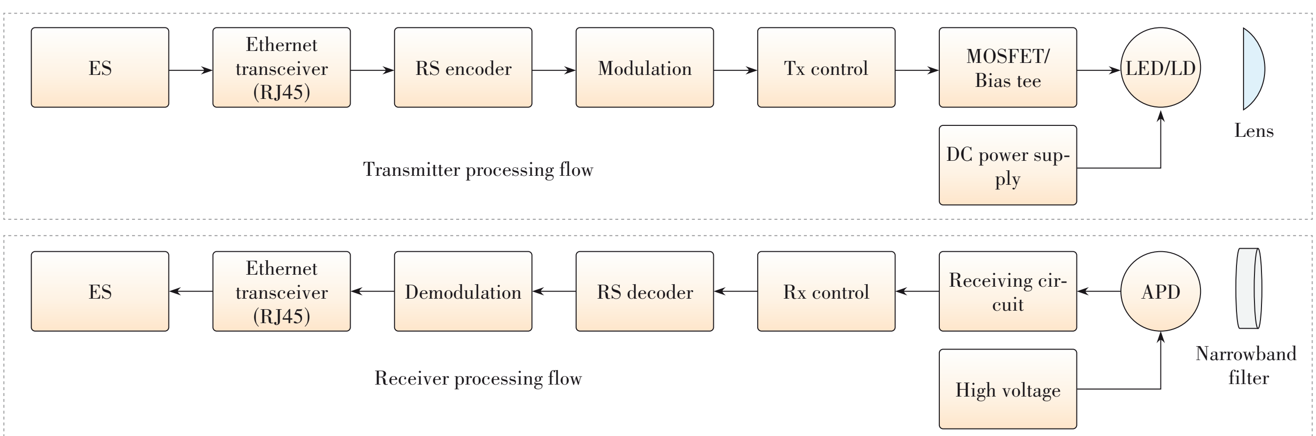

APD: avalanche photodiode
DC: direct current
ES: Ethernet switch
LD: laser diode
LED: light-emitting diode
MOSFET: metal-oxide-semiconductor field-effect transistor
RS: Reed-Solomon
Rx: receiver
Tx: transmitter

Figure 6. Transmission and reception principles of full-duplex optical communication systems

turned to the FPGA for decoding and demodulation. Subsequently, the processed signal is displayed on an external monitor through an RJ45 interface or transmitted to a Wi-Fi module for sharing.

As shown in Fig. 7a, a 20 Mbit/s pseudo-random binary sequence (PRBS) signal generated by an arbitrary waveform generator (AWG) replaces the FPGA signal at the TX to access the LC. After the signal decision at the RX, the output signal matches the original transmitted signal. The amplified analog signal from the first stage of the transimpedance amplifier (TIA) is captured, and the oscilloscope (Keysight, DSOS604A) generates the corresponding eye diagram, as depicted in Fig. 7b. This clear and open eye diagram confirms the accuracy of the received signal in Fig. 7a. The time and amplitude scales of the eye diagram are 20 ns and 500 mV, respectively, as shown in Fig. 7b. This method can also be applied to assess the communication performance of other optical communication system links.

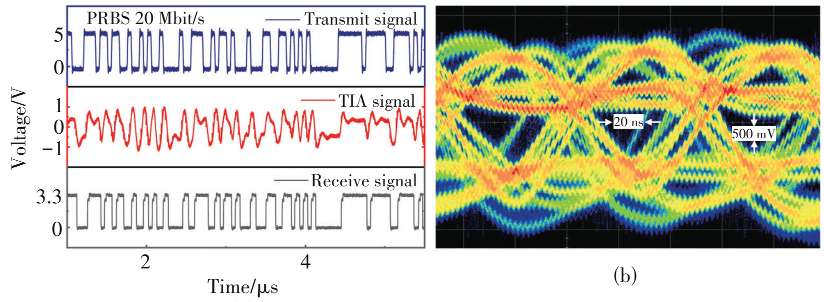

(a) (b)

PRBS: pseudo-random binary sequence TIA: transimpedance amplifier

Figure 7. (a) 20 Mbit/s PRBS signals from Rx of the system; (b) eye diagram of the analog signal output from TIA

In the WLC system, interference from ambient light is a primary challenge. To address this, we designed a bandpass filter tailored to the EL spectral peak of the white light LED lamp beads. This effectively suppresses background light interference, ensuring stable signal transmission.

In an underwater BLC system, rapid attenuation of light in water poses the greatest challenge. To mitigate this, we developed a specialized optical structure at the transmitter and adopt a three-window array design. These enhancements improve light transmission efficiency and signal coverage, significantly reducing signal attenuation in underwater environments.

For the DUVC system, the low light output efficiency of DUV LEDs is a major difficulty. To resolve this, we implemented sapphire substrate stripping technology and precise thinning of nitride films, enabling the production of sub-micron-level DUV LEDs. These advancements greatly enhance light output efficiency. Additionally, sunlight interference presents challenges for solar-blind communication. To address this, we designed a 275 nm bandpass filter at the receiver end, combined with an optical anti-reflection lens, which strengthened signal reception and effectively reduced signal attenuation during daytime communication in solar-blind regions.

Moreover, the primary challenge for LC systems lies in beam collimation. To overcome this, we optimized the optical system preceding the laser, ensuring precise beam alignment. This reduces the impact of atmospheric turbulence and beam divergence, enhancing communication stability and long-distance transmission capabilities.

Delay, packet loss rate (PLR), and jitter are three key metrics for evaluating the performance of an ALN. Delay refers to the time required for data to travel from one end of the network to the other. Increased delay may lead to stuttering during network interactions. PLR represents the proportion of data packets lost during transmission and reception. An increased PLR results in higher network delay and inefficient bandwidth utilization. Jitter refers to the inconsistency in packet delay during transmission, i.e., the arrival time variations of different data packets. Excessive jitter can disrupt data flow continuity, thereby compromising the smoothness of real-time communication.

The ALN contains five nodes. A PC is used as the accessing terminal, and a network camera serves as the accessed terminal. The delay measured under 25 different node access scenarios is shown in Fig. 8a by swapping their connection points. We used a maximum transmission unit of 1 514 bytes for testing. Due to the lower transmission rates of the BLC and WLC, these optical communication links introduced approximately 30 ms of delay, while the higher-speed DUVC and LC links resulted in a lower delay of around 6 ms. The same access setup was used to test the PLR and jitter of the ALN. As shown in Fig. 8b, as the number of nodes traversed increases,

Delay/ms		ALN accessed node				
		N1	N2	N3	N4	N5
ALN accessing node	N1	1.05	31.1	61.2	66.5	73.3
	N2	30.9	1.04	30.9	37.1	43.4
	N3	61.2	30.9	1.04	7.79	13.9
	N4	66.9	37.1	7.8	1.05	7.66
	N5	73.1	43.2	13.4	7.24	1.02

(a)

PLR/%		ALN accessed node				
		N1	N2	N3	N4	N5
ALN accessing node	N1	0	1	2.4	3.9	5.4
	N2	0.6	0	0.9	3	4.6
	N3	2.5	1.1	0	1.8	3.9
	N4	3.9	2.4	1.8	0	1.7
	N5	6.1	4.5	2.8	1.4	0

(b)

Jitter/ms		ALN accessed node				
		N1	N2	N3	N4	N5
ALN accessing node	N1	1	6	10	11	14
	N2	4	1	3	6	11
	N3	10	4	1	3	6
	N4	12	6	2	1	3
	N5	15	10	6	3	1

(c)

ALN: all-light network PLR: packet loss rate

Figure 8. (a) Delay, (b) PLR, and (c) jitter results of five nodes accessing each other

PLR accumulates steadily, with an average rise of 1.435% per optical link and a maximum PLR of 6.1%. Fig. 8c shows that the maximum jitter of 15 ms is measured when N5 accesses N1. Our testing results confirmed uninterrupted, high-quality real-time video transmission when the signal traveled along the longest path in the ALN (from N1 to N5).

3 Conclusions

By establishing an integrated communication network spanning space, air, and sea environments, we achieve full-duplex real-time video communication between network nodes, with a maximum PLR of 6.1% and transmission delay below 73.3 ms. The ALN system is designed to enable wireless internet access via the TCP/IP protocol. For Internet of Things (IoT) applications involving multi-terminal and multi-service interconnections, developing ALN-based mobile communication networks and integrating advanced modulation techniques to enhance network throughput will be crucial.

References

[1] SHAY T M, MACCANNELL J A, GARRETT C D, et al. First experimental demonstration of full-duplex communication on a single laser beam [C]//Proc. Free-Space Laser Communication and Active Laser Illumination III. SPIE, 2004. DOI: 10.1117/12.508511

[2] O'BRIEN D, TURNBULL R, MINH H L, et al. A 280 Mbit/s infra-red optical wireless communications system [C]//Proc. Free-Space and Atmospheric Laser Communications XI. SPIE, 2011. DOI: 10.1117/12.895092

[3] WANG K, NIRMALATHAS A, LIM C, et al. Experimental demonstration of a full-duplex indoor optical wireless communication system [J]. IEEE photonics technology letters, 2012, 24(3): 188 – 190. DOI: 10.1109/LPT.2011.2175912

[4] WANG K. Quasi-passive indoor optical wireless communication systems [J]. IEEE photonics technology letters, 2020, 32(21): 1373 – 1376. DOI: 10.1109/LPT.2020.3026343

[5] ABDALLA I, RAHAIM M B, LITTLE T D C. Interference in multi-user optical wireless communications systems [J]. Philosophical transactions of the royal society a: mathematical, physical and engineering sciences, 2020, 378(2169): 20190190. DOI: 10.1098/rsta.2019.0190

[6] TSONEV D, VIDEV S, HAAS H. Light fidelity (Li-Fi): towards all-optical networking [C]//Proc. Broadband Access Communication Technologies VIII. SPIE, 2013. DOI: 10.1117/12.2044649

[7] LI J, UYSAL M. Optical wireless communications: system model, capacity and coding [C]//Proc. IEEE 58th Vehicular Technology Conference (VTC 2003-Fall). IEEE, 2003: 168 – 172. DOI: 10.1109/VETECF.2003.1285000

[8] OUBEI H M, SHEN C, KAMMOUN A, et al. Light based underwater wireless communications [J]. Japanese journal of applied physics, 2018, 57 (8S2): 08PA06. DOI: 10.7567/JJAP.57.08PA06

[9] ROSHEIM M E, SAUTER G F. Free-space optical communications system pointer [C]//Proc. Free-Space Laser Communication Technologies XV. SPIE, 2003: 126 – 133. DOI: 10.1117/12.501653

[10] LIN A B, TONG Z, SONG Y H, et al. Underwater wireless optical communication system using blue LEDs [J]. Journal of physics: conference series, 2016, 679: 1 – 5. DOI: 10.1088/1742-6596/679/1/012032

[11] ARNON S. Underwater optical wireless communication network [J]. Optical engineering, 2010, 49(1): 1 – 6. DOI: 10.1117/1.3280288

[12] QI Z Q, WANG L N, LIU P Z, et al. Full-duplex underwater wireless blue light communication [J]. Optics express, 2023, 31(6): 9330 – 9338. DOI: 10.1364/oe.483966

[13] ZHOU Z H, YIN H X, YAO Y X. Wireless optical communication performance simulation and full-duplex communication experimental system with different seawater environment [C]//Proc. IEEE International Conference on Signal Processing, Communications and Computing (ICSPCC). IEEE, 2019. DOI: 10.1109/icspcc46631.2019.8960905

[14] WANG L N, BAI M M, QI Z Q, et al. Full-duplex wireless deep ultraviolet light communication [J]. Optics letters, 2022, 47(19): 5064 – 5067. DOI: 10.1364/OL.473369

[15] LIANG Y Z, WANG L N, QI Z Q, et al. Full-duplex wireless light communication using green laser diodes [J]. Optics express, 2024, 32(8): 13543 – 13551. DOI: 10.1364/oe.519815

Biographies

LIANG Yingze received his BS degree in communication engineering from East China Jiaotong University, China in 2022. He is currently working toward a master's degree in electronic information at Nanjing University of Posts and Telecommunications, China. His primary research interest lies in wireless optical communication and its application systems, including embedded development, communication electronics, and signal processing circuits.

WANG Linning received his BS degree in communications engineering and master's degree in electronics and communication engineering from Nanjing University of Posts and Telecommunications, China in 2018 and 2021, respectively. He is currently working toward a PhD degree in communication and information systems at Nanjing University of Posts and Telecommunications. His primary research interest lies in wireless optical communication and its application systems, including embedded development, communication electronics, and signal processing circuits.

QI Ziqian received his BS degree in electronic information engineering from Dalian Jiaotong University, China in 2021 and master's degree in electronics and communication engineering from Nanjing University of Posts and Telecommunications, China in 2024. His primary research interest lies in wireless optical communication and its application systems, including embedded development, communication electronics, and signal processing circuits.

LIU Pengzhan received his MS degree from Nanjing University of Posts and Telecommunications, China. Now he is a PhD student there under the supervision of Prof. WANG Yongjin. His research interests include all-light wireless optical communication networks and integrated GaN optoelectronic devices.

WANG Yongjin (wangyj@njupt.edu.cn) received his PhD degree in microelectronics and solid-state electronics from the Shanghai Institute of Microsystem and Information Technology, Chinese Academy of Sciences in 2005. He was engaged in research work with the University of Freiburg, Germany, Tohoku University, Japan, Forschungszentrum Jülich, Germany, and the University of Bristol, UK. Since 2011, he has been a professor with Nanjing University of Posts and Telecommunications, China. He is currently the chief investigator of the National Innovation Base for Micro-Nano Device and Information System, China. His research interests include III-nitride monolithic photonic circuits for visible light communication and the Internet of Things. He was the recipient of many scholarships, including the Humboldt Foundation Scholarship, the JSPS Special Researcher Scholarship, and the Royal Society for Engineering Scholarship.